Ultraviolet Irradiation of Nucleic Acids: Formation, Purification, and Solution Conformational Analyses of the Cis-Syn and Trans-Syn Photodimers of UpU†

Robert E. Rycyna‡ and James L. Alderfer*

Biophysics Department, Roswell Park Memorial Institute, Buffalo, New York 14263

Received July 20, 1987; Revised Manuscript Received December 14, 1987

ABSTRACT: Uridylyl(3′–5′)uridine (UpU) is subjected to aqueous acetone photosensitized radiation with sunlamps. These irradiation conditions form only cyclobutane-type photodimers. Purification of a specific configurational photodimer is accomplished by using C-18 reverse-phase high-performance liquid chromatography. Multinuclear NMR analysis is used to analyze photoproduct formation and to determine conformational features of these photodimers. Four photodimers are identified, with the cis-syn isomer predominant. The cis-syn and trans-syn photodimers of UpU exhibit markedly different furanose and exocyclic bond conformations. A comparison of the properties of the cis-syn dimers of UpU with those of dTpdT reveal many similar conformational features but also some that are different.

Frequent exposure to ultraviolet light can alter the biological properties of the constituent macromolecules in a living cell. The photochemical and photobiological effects of UV[1] light on nucleic acids [reviewed extensively by Wang (1976)] are of prime interest since they are crucial to cellular metabolism and their physicochemical properties enable the absorption of light in the UV-B region (290–320 nm), a portion of the solar spectrum. The formation of UV photoproducts is known to alter the structure and conformation of nucleic acids, which can subsequently interfere with processes such as DNA replication (Bollum & Setlow, 1963; Radman et al., 1977; Chan et al., 1985), transcription (Sauerbier, 1976), protein synthesis (Sarin & Johns, 1968), and endonucleolytic cleavage (Setlow et al., 1964; Hall & Larcom, 1982). Knowledge of the structural features of these altered nucleic acids will provide a more complete understanding of the biological effects of radiation-induced damage to cells and perhaps factors responsible for photolesion recognition by repair enzymes.

To ascertain the effect a photolesion has on the secondary structure of a nucleic acid helix, it is best to first understand the alterations induced into the sugar–phosphate backbone of a simple model such as the dinucleoside monophosphate. The ultraviolet photochemistry of various dinucleoside monophosphates has been reviewed extensively by Burr (1968), and conformational information has been obtained on some dinucleoside monophosphate photoproducts by using NMR spectroscopy and X-ray crystallography. Most studies focus on the most predominant photolesion formed in DNA and RNA, which is the cyclobutane-type pyrimidine photodimer (Fisher & Johns, 1976). Stereochemically, cyclobutyl-linked pyrimidines may exist in six configurationally distinct orientations, the most predominant being the cis-syn (CS) isomer (Varghese, 1972) (see Figure 1A). Trans-syn (TS) and cis-anti (CA) isomers exit as enantiomeric pairs whereas the trans-anti (TA) is a meso stereosiomer. Extensive NMR studies of the *cis-syn*-dT(p)dT photodimer (Hruska et al., 1975; Rycyna & Alderfer, 1985) revealed significant conformational changes in this photoproduct from d(TpT). The crystallographic structure of this same dT(p)dT dimer possessing a cyanoethyl phosphotriester linkage indicates some unexpected stereochemical changes associated with cis-syn dimer formation (Cadet et al., 1985). Production, isolation, and solution conformational analyses of additional isomeric dTpdT and dTpdC photodimers using ^{1}H NMR have also been reported by Liu and Yang (1978).

This report details the conformational investigations of ribodinucleoside monophosphates containing photodimers. RNA models are considered because they are photochemically very active, photodimers have been isolated from TMV RNA (Shuster, 1964), a photoreactivating enzyme has been found to act on TMV RNA (Bawden & Kleczkowski, 1959), and other repair mechanisms for RNA photolesions (Gordon et al., 1976) have been observed, thus supporting evidence for the biological importance of RNA photodimers. Furthermore, it has been suggested that a stretch of pyrimidine bases (...AUCACCUCCUUA-OH) at the 3′ terminus of *Escherichia coli* 16S rRNA forms several Watson–Crick hydrogen bonds with messenger RNA during the initiation of protein synthesis (Shine & Dalgarno, 1974; Steitz & Jakes, 1975). It can be expected that this polypyrimidine sequence would be highly susceptible to the photochemical action of ultraviolet light and that the conversion of such pyrimidine bases to cyclobutane photodimers would greatly alter the structure, the conformation, and the biological activity of the ribosome. Since CpC photodimers are unstable and are known to deaminate to UpU photodimers (Hariharan & Johns, 1968), the more relevant RNA model to investigate is UpU. The structural formula of a UpU photodimer [abbreviated as U(p)U] is shown in Figure 1B. Conformational features

† This work was supported by grants from the National Institutes of Health (CA39027 and 2T32-ES07057). Some of the NMR measurements were performed on an instrument purchased through grants from the Division of Research Resources of the NIH and from the Biophysics Program of the National Science Foundation. We acknowledge the financial support (to R.E.R.) of the SUNY/Buffalo Graduate Student Association.

* Author to whom correspondence should be addressed.

‡ Present address: Chemistry Department, Yale University, New Haven, CT 06511.

[1] Abbreviations: UpU, uridylyl(3′–5′)uridine; UV, ultraviolet; NMR, nuclear magnetic resonance; dT(p)dT, cyclobutane-type photodimers of dTpdT; U(p)U, cyclobutane-type photodimer of UpU; TnBAAc, tri-*n*-butylammonium acetate; TnBA(OH), tri-*n*-butylammonium hydroxide; ABC, ammonium bicarbonate; COSY, two-dimensional scalar-correlated spectroscopy; TMV, tobacco mosaic virus; EDTA, ethylenediaminetetraacetic acid; TBA, *tert*-butyl alcohol; TMP, trimethyl phosphate; U<>U, photodimer of uracil; Thy<>Thy, photodimer of thymine; DMT<>DMT, photodimer of 1,3-dimethylthymine.

0006-2960/88/0427-3142$01.50/0

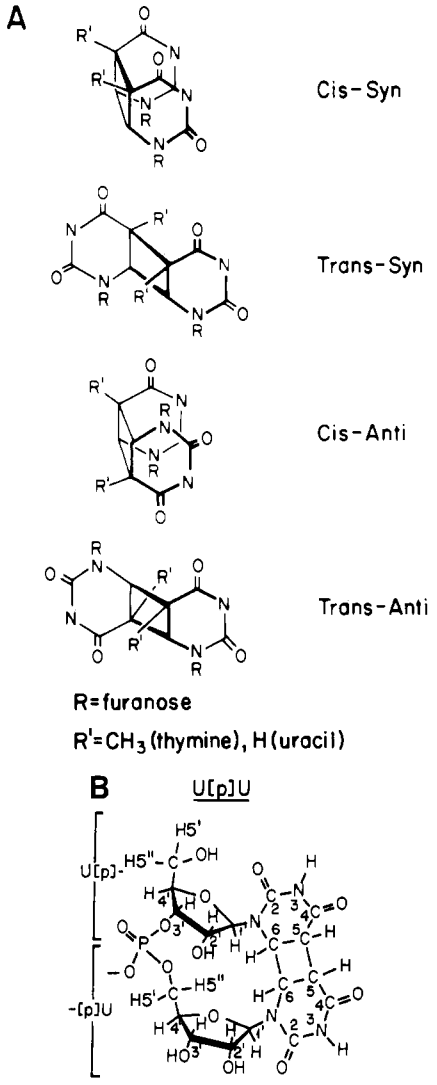

FIGURE 1: Structural formula of (A) pyrimidine bases in the cis-syn, trans-syn, cis-anti, and trans-anti configurations and (B) a UpU photodimer.

determined from these U(p)U photodimers will enable a comparison with their DNA analogue, dT(p)dT.

UpU is subjected to acetone-photosensitized irradiation conditions known to form only photodimers (Greenstock & Johns, 1968; Kucan et al., 1972); purification of the photodimers occurs by using C-18 reverse-phase HPLC. Conformational investigations of U(p)U photodimers is done by using multinuclear NMR techniques. These studies reveal that UV irradiation of UpU forms four photodimers, of which the most predominant is the cis-syn isomer. The *cis-syn-* and *trans-syn*-U(p)U photodimers have quite dissimilar furanose and exocyclic bond distributions. The different properties of both UpU photodimers may be responsible for inducing dissimilar alterations into an RNA helix. A comparison of the properties of the cis-syn dimers between UpU (from this work) and dTpdT (Rycyna & Alderfer, 1985; Cadet et al., 1985; Hruska et al., 1975) reveals many similar conformational features.

Materials and Methods

Materials. UpU was obtained from Sigma and 99.8% D_2O from Bio-Rad Laboratories.

UV Irradiation Sources. Four Westinghouse sunlamps (FS20T12) emitting an effective power spectrum of 310 ± 35 nm were used for photosensitized irradiations.

Acetone-Photosensitized Irradiation. Twenty-five milligrams of UpU was diluted to 1 mM in 30% aqueous acetone and transferred to a Pyrex Petri dish (9-cm diameter). The solution was irradiated with a UV fluence of 3.0 J/(m^2·s) under a nitrogen atmosphere at 2 °C until the sample received 250 kJ/m^2. Measurement of the UV fluence is done by using a long-wavelength Blak-Ray ultraviolet meter from UV Productions. Sample is maintained at 2 °C by placing Petri dishes on a $^1/_4$-in. aluminum plate, which is temperature controlled by a circulating coolant. UpU was converted almost quantitatively to photodimers after receiving 250 kJ/m^2 of UV light. Aqueous acetone was removed immediately by flash evaporation and the irradiated UpU resuspended in 0.2 mL of 100 mM TnBAAc (pH 7.4). The TnBAAc was prepared by titration of TnBA(OH) with acetic acid.

Chromatography of UpU Photoproducts. Twenty-five milligrams of UV-irradiated UpU was injected onto a 5-μm Ultrasphere (10 mm × 25 cm) semipreparative C-18 reverse-phase column and eluted isocratically with 100 mM TnBAAc at 1 mL/min. Separated photoproducts were desalted by loading onto a DEAE-Sephadex ion-exchange column and eluting with a linear gradient of H_2O to 0.25 M ABC (pH 8.1). Collected fractions were repeatedly flash evaporated to dryness to remove residual ABC.

NMR: Sample Preparation. ^{31}P NMR samples (10-mm tubes) were dissolved into 1.3 mL of 40% D_2O containing 4 mM EDTA (pH 7.0) and 10 mM TMP [used as internal chemical shift reference where $\delta(85\%\ H_3PO_4) = \delta(TMP) + 3.71$ ppm]. The concentration of U(p)U-1 (described under Results) was about 25 mM while that of U(p)U-2 was 7.0 mM. ^{13}C NMR samples (in 5-mm tubes) were prepared in a similar fashion with the exceptions that dioxane was the internal reference and the final volume was 0.4 mL. Sample concentrations for ^{13}C NMR studies were 76 (U(p)U-1) and 23 mM (U(p)U-2). ^1H NMR samples were lyophilized 2 times from 99.8% D_2O, dissolved into 0.35 mL of 99.8% D_2O containing either U(p)U-1 (88 mM) or U(p)U-2 (27 mM) and 0.5 mM EDTA (pH 7.38), 5 mM NaH_2PO_4 (pH 7.4), and 10 mM TBA, and transferred into 5-mm tubes. Proton chemical shift values are reported relative to internal sodium 3-(trimethylsilyl)[2,2,3,3-^{2}H]propionate (TSP) where $\delta(TSP) = \delta(TBA) + 1.2542$ ppm at 30 °C. The pH_{obsd} is the pH meter reading of solutions containing D_2O. Unless specifically mentioned, all ^1H, ^{13}C and ^{31}P chemical shift values are reported at 30 °C.

NMR: Conventional Acquisitions. ^{31}P NMR data was recorded by a Bruker WP-200 (80.961 MHz) operating in the pulsed Fourier transform (FT)/quadrature phase acquisition mode. Field stabilization was maintained by internal locking to the deuterium resonance of the solvent. Free-induction decay (FID) data were accumulated and transformed by an Aspect 2000 minicomputer. ^{31}P spectra were recorded after using an inverse-gated routine [proton decoupled without nuclear Overhauser effect (NOE)] or a gated sequence (proton coupled with NOE). Total pulse cycle time in the inverse-gated routine was 7.05 s. This effectively permits complete relaxation of the phosphorus nuclei in order to obtain accurate peak areas. ^{13}C NMR spectra were recorded by a Bruker AM-400 (100.621 MHz) using broad-band proton decoupling. ^1H NMR data were acquired on our own Bruker AM-400 (400.135 MHz), a Bruker AM-500 (500.138 MHz) at Bruker Spectrospin, Ltd. (Canada), and the WP-500 (500.136-MHz) spectrometer at the Chemical Instrumentation Center, Yale University.

NMR: Two-Dimensional (2-D) COSY Acquisitions. A pulse sequence $90°-t_1-90°-\mathrm{FID}(t_2)$ was used. 2-D COSY data sets consisted of 512 data points along t_1 and 2048 points

Table I: Distributions and ^{31}P NMR Chemical Shift Values[a] of UpU Photoproducts[b]

product	% yield	ratio[c]	18 °C	30 °C	63 °C	$\Delta\delta$[d]
UpU	0.0		-3.785	-3.679	-3.493	0.292
U(p)U-1	70.7	7.7	-4.696	-4.657	-4.612	0.084
U(p)U-2	10.6	1.2	-3.921	-3.887	-3.885	0.036
U(p)U-3	9.5	1.0	-3.259	-3.211	-3.198	0.061
U(p)U-4	9.2	1.0	-4.079	-4.002	-3.885	0.194

[a] Chemical shift values in ppm (±0.005) from internal TMP. [b] Photosensitized irradiation in 30% aqueous acetone at 2 °C with 250 kJ/m^2 of 310-nm light. [c] Ratio is photoproduct yield normalized to yield of U(p)U-4. [d] $\Delta\delta = \delta(60\ °C) - \delta(18\ °C)$.

along t_2 with spectral widths of 950 and 1900 Hz, respectively. Digital resolution was 1.85 Hz/point along t_1 and 0.925 Hz/point along t_2. Sixteen transients were accumulated for each value of t_1 with a 2.0-s delay between observation pulses. A 16-step phase-cycling procedure for quadrature detection suppressed phantom peaks. Data matrix was zero-filled to 1024 points along t_1, and then both dimensions were multiplied by a sine bell function. After 2-D fourier transformation, the data matrix was symmetrized.

Spectral Simulations. ^1H NMR parameters listed in Table II for *cis-syn-* and *trans-syn*-U(p)U were refined by using the iterative spin-simulation program PANIC.[2] Simulations were performed on proton NMR data obtained at both 200 and 500 MHz. The calculated errors of the parameters were usually between 0.09 and 0.12 Hz for 600–800 transitions. After individually simulated furanose and base proton spin systems received an appropriate line-broadening treatment, they were added together in order to obtain a complete proton spectrum of the molecule.

RESULTS

The sensitivity of the phosphorus chemical shift value to the O–P–O bond angle and torsion angles α(P–O5′) and ξ(O3′–P) in nucleic acids (Gorenstein, 1978) enables ^{31}P NMR to be exploited as a qualitative probe of sugar–phosphate backbone distortion in UV-irradiated nucleic acids. Prior to irradiation of UpU, the ^{31}P NMR spectrum shows one resonance at −3.68 ppm for unmodified UpU. The distribution and ^{31}P NMR chemical shift values of UpU photoproducts after sensitized irradiation are found in Table I. These data indicate that irradiation of UpU forms four major photoproducts possessing different ^{31}P chemical shift values and the UpU is quantitatively converted to photoproducts. Table I also lists the temperature dependence of the ^{31}P chemical shift values between 18 and 63 °C. Clearly, all four products have smaller temperature dependency compared with UpU. Since the ^{31}P chemical shift value of a rigid nucleotide such as 3′,5′-cUMP is temperature independent between 18 and 63 °C (unpublished results) and is attributed to constrained phosphodiester angles (Gorenstein, 1978), the small temperature-dependent chemical shift values for UpU photoproducts are consistent with a "more rigid" phosphodiester region constrained by a cyclobutane ring. Reirradiation of each of the four photoproducts with 254-nm light and comigration with UpU on TLC support their assignment as photodimers. The photodimer ratio of 7.7:1.2:1:1 (Table I) determined immediately following irradiation is reasonably similar to the 6:2:1 ratio observed by Brown et al. (1966) for U(p)U photodimers after direct irradiation with 265-nm light.

[2] PANIC (Parameter Adjustment in NMR by Iterative Calculation) is a minicomputer version of the LAOCOON-type programs, provided in the software packages of the Bruker NMR spectrometers by Bruker Instruments, Inc., Billerica, MA.

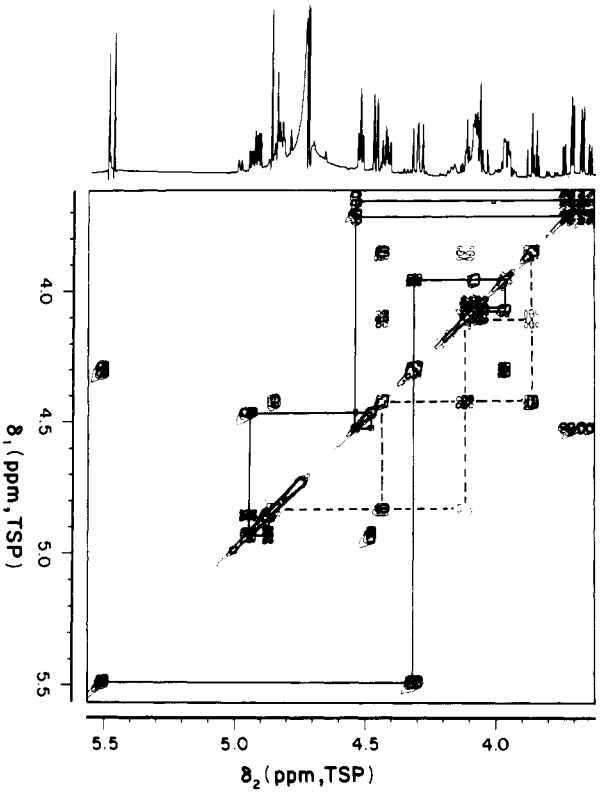

FIGURE 2: Contour plot of 400-MHz 2-D COSY spectrum of U(p)U-1 at 24 °C in D_2O. Furanose proton scalar interactions are shown by solid lines, and dashed lines indicate base proton connectivities.

Purification of U(p)U photodimers was achieved by C-18 reverse-phase high-performance liquid chromatography (HPLC). Only three fractions (called A, B, and C) are separated adequately as determined by ^{31}P NMR: fraction A showed a ^{31}P NMR resonance at −4.66 ppm, U(p)U-1, and −3.21 ppm, U(p)U-3, in a ratio of 8.4:1.0; fraction B displayed a single resonance at −3.89 ppm corresponding to U(p)U-2; and fraction C had a very small resonance at −3.68 ppm indicative of UpU. Although a small percent of U(p)U-3 was observed to elute with U(p)U-1, the former was never purified to the degree necessary to warrant further NMR spectroscopic studies. Critical pursuit of the remaining minor photoproduct, U(p)U-4, was not undertaken.

Solution conformational investigations of the isolated UpU photodimers, U(p)U-1 and U(p)U-2, were initiated by using ^1H NMR. The proton NMR patterns of U(p)U-1 reveal highly unusual features for a ribodinucleoside monophosphate. Figure 2 shows the resolution-enhanced 1-D 400-MHz ^1H NMR spectrum and 2-D COSY contour plot of U(p)U-1. Scalar-coupled furanose protons are connected by solid lines while the saturated base H5–H5, H5–H6, and H6–H6 interactions are highlighted by the dashed lines. The H1′ protons are identified as doublets at 4.86 and 5.49 ppm. The COSY spectrum shows a strong interaction between the upfield H1′ (4.86 ppm) and an H2′ at 4.93 ppm. The H2′ correlates with H3′ at 4.47 ppm which, in turn, has a weak off-diagonal peak to the H4′ (4.53 ppm). Very intense cross-peaks are observed between the H4′ and both H5′ and H5″ at 3.72 and 3.66 ppm, respectively. Assignment of these six correlated protons to the U(p)-nucleotide is made for three reasons. First, a phosphorus interaction is observed to the H3′ (4.47 ppm) in Figure 3 (top); the interaction is removed in the presence of broad-band phosphorus decoupling (Figure 3, bottom). Second, the chemical shift positions of the H5′ and H5″ are characteristic of a 5′-terminal ribofuranose. Finally, there is no evidence

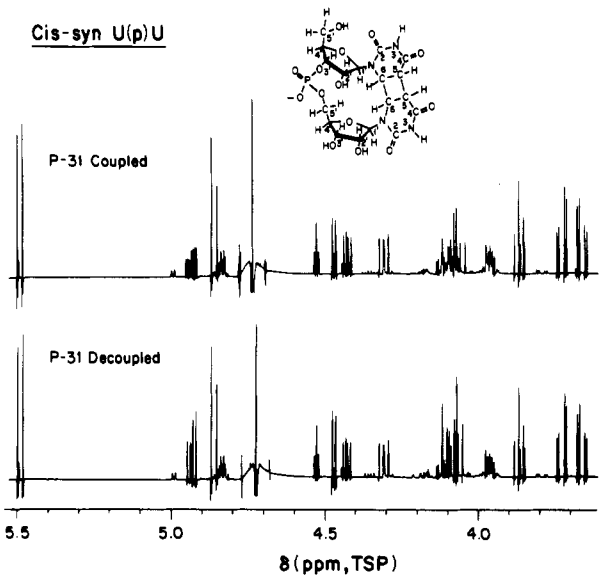

FIGURE 3: 500-MHz proton NMR spectra of *cis-syn*-U(p)U in D_2O at 30 °C (top) with ^1H–^{31}P interactions and (bottom) without ^1H–^{31}P interactions by broad-band phosphorus decoupling.

in these H5′ and H5″ multiplets of coupling to the phosphorus atom (Figure 3). The proton NMR parameters for this nucleotide were refined by computer simulation using PANIC. Assignment of the U(p)- H5′, H5″ methylene protons is made by the convention that H5″ resonates to higher field (Remin & Shugar, 1972) and is consistent with the method of Hruska et al. (1975) for the predominant *cis-syn*-dT(p)dT photodimer. The other ribofuranose H1′ (5.49 ppm) is scalar correlated to the H2′ at 4.31 ppm and then to the H3′ (3.96 ppm). The remaining connectivities indicate the H4′, H5′, and H5″ are severely overlapped in a region between 4.05 and 4.13 ppm. Assignment of these furanose protons to the -(p)U fragment is made because a phosphorus interaction with the H3′ (3.97 ppm) is not observed in Figure 3 (top) as expected for a terminal 3′-nucleotide [i.e., -(p)U]. ^1H NMR parameters for the H1′, H2′, and H3′ protons on the -(p)U fragment were refined by computer simulation, but the tightly coupled ABC spin system (H4′, H5′, H5″), further complicated by an interaction between each proton and the phosphorus atom, prevented completion of this furanose system.

The potential to extract additional information from the proton NMR data of U(p)U-1 is limited due to some unexpected chemical shift positions, the severe resonance overlap in the 4.05–4.13 ppm region, and many uncanny multiplet patterns. Nevertheless, broad-band phosphorus decoupling (Figure 3, bottom) did aid in simplifying some difficulties and provided more structural information about the molecule. The decoupling changes three regions. First, the U(p)- H2′ multiplet at 4.93 ppm simplifies from a pattern of seven lines to four lines, which indicates a highly unusual situation; namely, an H2′ in a 3′→5′ phosphodiester has a scalar interaction with the phosphorus atom. Second, the U(p)- H3′ at 4.46 ppm shows $J_{H3',P}$ = 1.03 Hz, thereby suggesting conformational changes in the exocyclic bond ϵ(C3′–O3′), which will be discussed later. Finally, although the patterns of the -(p)U H4′, H5′, and H5″ protons were simplified, computer simulation of their parameters still could not be accomplished because of the complex virtual coupling situation. The top and bottom panels of Figure 3 also show resonances belonging to U(p)U-3; however, their presence does not influence the spectral characteristics of U(p)U-1.

Four heterocyclic base protons in U(p)U-1 are identified by scalar cross-peaks connected by dashed lines in the COSY spectrum. Typically, these H5 and H6 protons in unmodified UpU belong to unsaturated heterocyclic rings and resonate further downfield (5.88 and 7.93 ppm, respectively). The large upfield shifts experienced by these base protons in the formation of U(p)U-1 are characteristic of C5=C6 saturation (Kan et al., 1982). Figure 2 indicates a variety of scalar connectivities between four base protons at 4.84, 4.44, 4.12, and 3.87 ppm. Refinement of the chemical shift values and coupling constants of these base protons was accomplished by computer simulation. The H5 and H6 protons are assigned by a similarity of parameters with analogous protons on the *cis-syn*-dT(p)dU photodimer reported by Liu and Yang (1978). The proton at 4.44 ppm is assigned as the U(p)- H6 because of a chemical shift similarity with the dT(p)- H6 at 4.49 ppm in dT(p)dU. The protons at 4.84 and 3.87 ppm are assigned as the -(p)U H6 and H5, respectively, due to a chemical shift resemblance with the -(p)dU H6 and H5 protons at 4.71 and 3.63 ppm in dT(p)dU. The remaining proton at 4.12 ppm is assigned by default to the U(p)- H5. The coupling constants determined for U(p)U-1 base protons (9.77, −2.74, 9.35, 4.86, and −7.32 Hz) are similar in magnitude to the $J_{H5,H5}$ (9.31 Hz), $J_{H5,H6*}$ (1.70 Hz), $J_{H5,H6}$ (7.92 Hz), and $J_{H6,H6}$ (4.21 Hz) observed by Liu and Yang (1978) for the cis-syn 1,3-dimethyluracil photodimer. The minor variation between these coupling constants probably results from a small change in the conformation but not the configuration of the cyclobutane ring.

Assignment of U(p)U-1 as the *cis-syn*-U(p)U photodimer is made because of (1) the similarity of the base proton parameters (Table II) with models examined by Liu and Yang (1978), (2) the formation of predominantly U(p)U-1 as observed by Brown et al. (1966), and (3) the large upfield shift in the ^{31}P resonance of UpU to U(p)U-1 (Table I) similar to the shift in the formation of *cis-syn*-dT(p)dT from dTpdT (Rycyna & Alderfer, 1985).

The ^1H NMR parameters for UpU and *cis-syn*-U(p)U are compared in Table II; parameters quoted to less significant digits were not completely refined by computer simulation but only approximated by first-order analysis. The upfield shift of the U(p)- H1′ is characteristic of the formation of a cis-syn photodimer (Hruska et al., 1975; Liu & Yang, 1978); however, the magnitude of the shift (1.03 ppm) is quite large when compared with deoxyphotodimers (0.3–0.6 ppm). The U(p)- H2′ has undergone a 0.47 ppm shift downfield similar in magnitude (0.3 ppm) and direction to the *cis-syn*-dT(p)- H2′ observed in the dTpdT to *cis-syn*-dT(p)dT conversion (Hruska et al., 1975; Rycyna & Alderfer, 1985). The U(p)- H3′, H4′, H5′, and H5″ underwent minor modulations in chemical shift positions. Most of these U(p)- furanose protons experienced chemical shift value changes similar to those observed in the conversion of dTpdT to *cis-syn*-dT(p)dT. Alterations in many coupling constants reflect very significant conformational distortions. The large increase in $J_{1'2'}$ from 4.2 to 8.98 Hz in conjunction with the much-reduced $J_{3'4'}$ from 5.0 to 0.87 Hz indicates a strong bias for a C2′-endo sugar pucker. The $J_{2'3'}$ remains unchanged while the $J_{4'5'}$ increases to 3.31 Hz and the $J_{4'5''}$ decreases to 3.59 Hz. Two observations suggest other radical conformational redistributions in the phosphodiester region. First, $J_{p3'}$ undergoes a severe reduction from 8.2 Hz in UpU to 1.1 Hz in *cis-syn*-U(p)U. Second, the scalar interaction of the phosphorus atom and U(p)- H2′ at 4.93 ppm (shown in Figure 3) was totally unexpected; the magnitude of the four-bonded $J_{p2'}$ is 2.95 Hz.

Formation of *cis-syn*-U(p)U induces changes in the -(p)U nucleotide. The H1′ is shifted 0.47 ppm upfield to 5.49 ppm,

Table II: ^{1}H NMR Parameters[a] for UpU and *cis-syn-* and *trans-syn*-U(p)U Photodimers

	UpU[b]		*cis-syn*-U(p)U		Δδ[c]		*trans-syn*-U(p)U		Δδ[d]	
parameter	Up-	-pU	U(p)-*	-(p)U	Up-	-pU	U(p)-*	-(p)U	Up-	-pU
H1′	5.892	5.950	4.860	5.488	−1.032	−0.462	5.849	4.891	−0.043	−1.059
H2′	4.461	4.342	4.932	4.307	0.471	−0.035	4.683	4.582	0.222	0.240
H3′	4.553	4.346	4.470	3.965	−0.083	−0.381	4.587	4.638	0.034	0.292
H4′	4.338	4.272	4.527	4.07	0.189	−0.20	3.993	3.947	−0.345	−0.325
H5′	3.942	4.284	3.724	4.10	−0.218	−0.18	3.936	4.210	−0.006	−0.074
H5″	3.845	4.140	3.663	4.06	−0.182	−0.08	3.919	4.134	0.074	−0.006
H5	5.869	5.896	4.119	3.871	−1.750	−2.025	3.490	3.562	−2.379	−2.334
H6	7.931	7.936	4.443	4.839	−3.488	−3.097	5.057	4.752	−2.874	−3.184
$J_{1'2'}$	4.2	3.9	8.98	8.23			<0.30	1.66		
$J_{2'3'}$	5.2	5.1	5.29	6.85			5.64	6.04		
$J_{3'4'}$	5.3	5.0	0.87	3.81			9.73	8.77		
$J_{4'5'}$	2.4	2.4	3.31	4.9			2.18	2.63		
$J_{4'5''}$	4.0	3.2	3.59	0.1			2.45	4.55		
$J_{5'5''}$	−13.1	−11.9	−12.33	−11.9			−13.33	−11.88		
$J_{p2'}$			2.95							
$J_{p3'}$	8.2		1.08				9.74			
$J_{p4'}$		2.0		*e*				1.64		
$J_{p5'}$		4.4		2.38				9.07		
$J_{p5''}$		4.5		8.14				5.16		
J_{5*5}			9.77				3.02			
J_{5*6}			−2.74				−1.41			
J_{5*6*}			9.35				9.19			
J_{56*}			−7.32				−1.41			
J_{66*}			4.86				7.99			
J_{56}	8.1	8.2	0.00				9.19			

[a] Chemical shift values (δ) in ppm (±0.0003) from TSP; coupling constants (*J*) in Hz (±0.15). Data accumulated in D_2O at 30 °C. [b] Data accumulated in D_2O at 18 °C from Lee et al. (1976). [c] Δδ = δ[*cis-syn*-U(p)U] − δ(UpU). [d] Δδ = δ[*trans-syn*-U(p)U] − δ(UpU). [e] Value not determined due to severe resonance overlap and pattern complexity.

Table III: ^{13}C NMR Parameters[a] for UpU and *cis-syn-* and *trans-syn*-U(p)U Photodimers

	UpU		*cis-syn*-U(p)U		Δδ[b]		*trans-syn*-U(p)U		Δδ[c]	
parameter	Up-	-pU	U(p)-	-(p)U	Up-	-pU	U(p)-	-(p)U	Up-	-pU
$\delta_{C1'}$	22.66	22.49	24.89	19.98	2.23	−2.51	23.13	31.57	0.47	9.08
$\delta_{C2'}$	6.32	7.18	0.89	2.34	−5.43	−4.84	8.14	6.56	1.82	−0.62
$\delta_{C3'}$	6.50	2.73	8.70	1.54	2.20	−1.19	4.25	1.83	−2.25	−0.90
$\delta_{C4'}$	16.86	16.12	13.52	14.64	−3.34	−1.48	14.03	13.85	−2.83	−2.27
$\delta_{C5'}$	−6.23	−2.04	−4.94	−0.19	1.29	1.85	−2.04	−5.36	4.19	−3.32
δ_{C2}	85.04[d]	85.01	85.68[d]	87.88	0.64	2.87	86.51[d]	84.96	1.47	−0.05
δ_{C4}	99.48[d]	99.42	101.54[d]	103.70	2.06	4.28	105.49[d]	105.45	6.01	6.03
δ_{C5}	35.82[d]	35.67	−23.30	−32.23	−59.12	−67.90	−26.51[d]	−26.72	−62.33	−62.39
δ_{C6}	74.93[d]	74.79	−5.56	−18.47	−80.49	−93.26	−8.04	−14.96	−82.97	−89.75
$J_{pC2'}$	4.2		8.8				4.9			
$J_{pC3'}$	5.2		6.1				5.7			
$J_{p3'C4'}$	4.7		<0.5				5.7			
$J_{p5'C4'}$		8.7		7.6				3.6		
$J_{pC5'}$		5.3		5.3				5.7		

[a] Chemical shift values (δ) in ppm (±0.002) from dioxane; coupling constants (*J*) in Hz (±0.23). Data accumulated in D_2O at 30 °C. [b] Δδ = δ[*cis-syn*-U(p)Y] − δ(UpU). [c] Δδ = δ[*trans-syn*-U(p)U] − δ(UpU). [d] Base carbon resonances not assigned unambiguously.

which is similar in magnitude and direction to the 0.32 ppm shift observed in the dTpdT to *cis-syn*-dT(p)dT conversion. The H2′ remains virtually unchanged but the H3′ moves upfield 0.38 ppm, which is similar to the 0.26 ppm shift of H3′ in *cis-syn*-dT(p)dT (Rycyna & Alderfer, 1985). The -(p)U H4′, H5′, and H5″ move upfield 0.08–0.20 ppm. Conformational alterations are also evident in the -(p)U furanose. The large increase in $J_{1'2'}$ from 3.9 to 8.23 Hz and decrease in $J_{3'4'}$ from 5.0 to 3.81 Hz suggests a preference for C_2'-endo. The $J_{2'3'}$ increases moderately from 5.1 to 6.68 Hz. The $J_{p5'}$ and $J_{p5''}$, which are obtained from a comparison of the phosphorus-coupled and proton-decoupled spectra (top and bottom panels of Figure 3), reveal a decrease from 4.4 to 2.38 Hz and a large increase from 4.5 to 8.14 Hz, respectively. The $J_{p4'}$ was unable to be estimated due to the resonance overlap.

Carbon-13 NMR parameters for *cis-syn*-U(p)U are compared with those for UpU in Table III. Assignment of every protonated carbon is made unequivocally by using the ^{13}C off-resonance decoupling technique following assignments of the proton spectrum; however, carbonyl carbon assignments between nucleotide units are tentative. A variety of chemical shift value changes occur in the U(p)- fragment due to the conversion of UpU to *cis-syn*-U(p)U. Alterations worth noting include (1) a downfield shift of C1′ from 22.66 to 24.89 ppm, (2) a 5.4 ppm upfield shift in the C2′, and (3) an upfield shift for C4′. Excluding the 2.5 ppm upfield shift of the -(p)U C1′, these shifts for all furanose carbons are consistent with those in the dTpdT to *cis-syn*-dT(p)dT conversion (Rycyna & Alderfer, 1985). However, the C2 and C4 carbonyl carbons in both nucleotides experience a smaller deshielding than the same carbons in *cis-syn*-dT(p)dT. As expected, the C5 and C6 carbons undergo significant upfield shifts reflecting C5=C6 bond saturation.

The carbon–phosphorus coupling constants of *cis-syn*-U(p)U (Table III) indicate conformational changes in the phosphodiester region and exocyclic bonds as supported by the proton NMR results. The very large increase (4.6 Hz) in U(p)- $J_{pC2'}$ and large decrease (4.2 Hz) in U(p)- $J_{pC4'}$ corroborates with

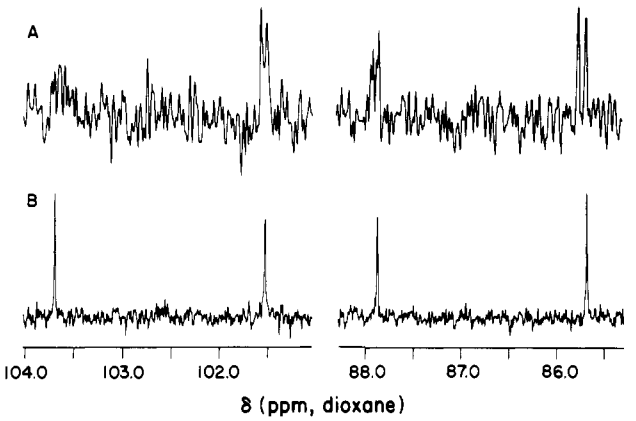

FIGURE 4: 100.621-MHz carbon-13 NMR subspectra of *cis-syn*-U-(p)U at 30 °C: (A) proton coupled and (B) broad-band proton decoupled.

the large $J_{1'2'}$, the very small $J_{3'4'}$, and the appearance of a four-bonded $J_{p2'}$. Other changes in $J_{C,P}$ values include an increase in $J_{pC3'}$ from 5.2 to 6.1 Hz and a decrease in -(p)U $J_{pC4'}$ from 8.7 to 7.6 Hz. Conformational changes reflected in the coupling constants for *cis-syn*-U(p)U (Table III) are reasonably consistent with those observed in the conversion of dTpdT to *cis-syn*-dT(p)dT with the exception of the major reduction in $J_{p3'C4'}$.

The existence of a cyclobutane ring pucker as observed in the crystal structure of *cis-syn*-U<>U (Adman & Jensen, 1970) in addition to the orientations about the glycosyl bonds were investigated in *cis-syn*-U(p)U by using proton-coupled carbon-13 NMR. Figure 4 shows the ^{13}C NMR subspectra of the carbonyl region obtained (A) with proton coupling and (B) with broad-band proton decoupling. The spectra illustrate different patterns for the C2 carbons at 85.7 and 87.9 ppm. Unambiguous assignments of the coupling constants have not been made; however, the patterns qualitatively reveal contrasting torsion angles between C2–H1′ and C2–H6 atoms belonging to different nucleosides. Figure 4A also shows considerably dissimilar C4 carbon patterns (101.5 and 103.7 ppm).

Conformational investigations of the other isolated UpU photoproduct, U(p)U-2, were initiated by using proton NMR. Figure 5A,C,E,G shows the 500-MHz ^1H NMR subspectra of U(p)U-2. Resonance assignments were aided by using the 2-D COSY technique. All furanose and base proton NMR parameters for U(p)U-2 were approximated by a first-order analysis and then refined by using PANIC; Figure 5B,D,F,H shows the computer-simulated subspectra of U(p)U-2. Features observed in these ^1H parameters provided for the identification of the cyclobutane ring configuration. The chemical shift values of three base protons in U(p)U-2 (3.56, 4.75, and 5.06 ppm) are observed to be similar to the UH5 (3.51 ppm), UH6 (4.58 ppm), and TH6 (4.67 ppm) reported for the trans-syn II dT(p)dU photodimer (Liu & Yang, 1978). They also reported the coupling constants for trans-syn 1,3-dimethyluracil photodimer to be 2.81 (J_{5*5}), 9.79 (J_{56}), −1.63 (J_{56*}), and 7.01 Hz (J_{66*}). The coupling constants observed in U(p)U-2 are 3.02, 9.19, −1.41, and 7.99 Hz, which are in quite good agreement with (1) those values for *trans-syn*-U<>U, (2) the J_{56} (8.7 Hz) and J_{66*} (7.5 Hz) for the dT(p)dU photodimer (Liu & Yang, 1978), and (3) $J_{H5,H6}$ (9.5–10.2 Hz) from trans-substituted 5,6-dihydrouracil compounds (Katritzky et al., 1969). The minor variation in coupling constants between these values may reflect an insignificant change in the conformation of the cyclobutane ring. Therefore, the NMR data suggests U(p)U-2 possesses the trans-syn cyclobutyl

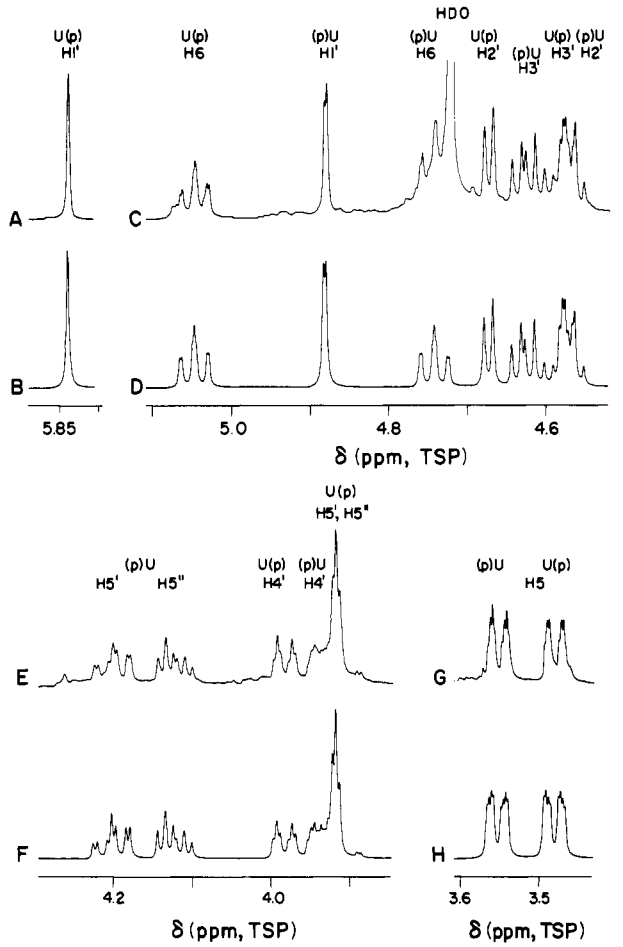

FIGURE 5: 500-MHz proton NMR data of U(p)U-2 in D_2O at 30 °C. Subspectra A, C, E, and G are experimental data, and subspectra B, D, F, and H are simulated data.

configuration because the proton parameters for the base protons in U(p)U-2 are very similar to those observed for the trans-syn II uracil photodimer (Liu & Yang, 1978) and the ^{31}P NMR chemical shift value of U(p)U-2 (−3.887 ppm) is similar to that of the trans-syn I dT(p)dT (−3.976 ppm) observed by Rycyna and Alderfer (1985).

The refined ^1H NMR parameters for *trans-syn*-U(p)U are compared with those of UpU and *cis-syn*-U(p)U in Table II. Notable chemical shift changes in the furanose protons of the U(p)- fragment are reflected by the significant downfield shift (0.22 ppm) of H2′ and upfield shift (0.35 ppm) of H4′. The chemical shift values of the other U(p)- protons remain essentially unchanged with the exception of the large upfield shift in H5 and H6, a consequence of ring saturation. Significant conformational alterations are observed in the U(p)- furanose as suggested by some unusual coupling constants. There is a drastic reduction of $J_{1'2'}$ from 4.2 to less than 0.30 Hz and a large increase in $J_{3'4'}$ from 5.3 to 9.73 Hz. The U(p)- $J_{2'3'}$ and $J_{4'5'}$ change little, but the $J_{4'5'}$ reduces moderately from 4.0 to 2.45 Hz. The large increase in $J_{p3'}$ to 9.74 Hz has conformational implications for exocyclic bond ϵ(C3′–O3′), to be discussed later.

The chemical shift value changes in the -(p)U fragment also indicate large alterations in that moiety. In contrast to *cis-syn*-U(p)U, where the U(p)- H1′ was shifted far upfield, it is the -(p)U H1′ in *trans-syn*-U(p)U that moves upfield 1.06 ppm. The -(p)U H2′ and H3′ both move downfield almost 0.3 ppm while the H4′ is shifted 0.33 ppm upfield. The furanose distribution is modified due to the decrease in -(p)U $J_{1'2'}$ from 3.9 to 1.66 Hz and the increase in $J_{3'4'}$ from 5.0 to

Table IV: Furanose Distributions for UpU and *cis-syn*- and *trans-syn*-U(p)U

			equilibrium[d]							
			form I			form II				
	% C2′-endo[a]	% C3′-endo[b]	f_I	P_I	C_I	f_{II}	P_{II}	C_{II}	Φ	error (Hz)[e]
UpU										
Up-	44 (42)[c]	56	0.57	−20.1	$_2E$	0.43	137.5	$_1T^2$	40.0	0.19
-pU	43 (39)[c]	57	0.59	−18.9	$_2E$	0.41	151.0	$^2T_1$	38.0	0.19
cis-syn-U(p)U										
U(p)-	91 (90)[c]	9	1.00	153.4	$^2T_1$	0.0			41.8	0.71
-(p)U	68 (82)[c]	32	1.00	125.1	$_1E$	0.0			40.5	0.48
trans-syn-U(p)U										
U(p)-	3 (23)[c]	97	1.00	20.4	^3E	0.0			38.0	2.30
-(p)U	16 (17)[c]	84	1.00	30.6	$^3T_4$	0.0			33.2	0.27

[a] Equation used: $f_{C2'\text{-endo}} = J_{1'2'}/(J_{1'2'} + J_{3'4'})$, from Alderfer and Ts'o (1977). [b] Equation used: $f_{C3'\text{-endo}} = J_{3'4'}/(J_{1'2'} + J_{3'4'})$, from Alderfer and Ts'o (1977). [c] Equation used: $f_{C2'\text{-endo}} = 10J_{1'2'}$, from Altona and Sundaralingam (1973). [d] Calculations are performed by using the program PSEUROT. The data are analyzed by assuming a two-state equilibrium (consisting of mole fractions f_I and f_{II}), with an amplitude of pucker Φ and phase angles P_I and P_{II} (deg); C_I and C_{II} are the corresponding envelope or twist notation that classify the sugar puckering modes (Altona & Sundaralingam, 1973). [e] This is the sum of the differences (absolute value) between the experimental furanose coupling constants and their calculated values.

8.77 Hz. Alterations in the phosphodiester region are reflected in the large increase in $J_{p5'}$. A comparison of the proton NMR parameters between *cis-syn*-U(p)U and *trans-syn*-U(p)U (Table II) indicates a variety of different conformational properties in these UpU photodimers.

Carbon-13 NMR parameters obtained for *trans-syn*-U(p)U are compared with those for UpU and *cis-syn*-U(p)U in Table III. Assignment of every protonated carbon has been made with the exception of the C5 carbons by using the ^{13}C off-resonance technique following the assignment of the proton spectrum. A variety of changes in chemical shift values are described for both furanose systems. The -(p)U C1′ experiences a significant downfield shift (9.1 ppm) whereas the U(p)-C1′ remains unchanged. The C2′, C3′, and C4′ in both furanose fragments undergo modulations in their chemical shift values. The U(p)- C5′ moves downfield 4.2 ppm, and the -(p)U C5′ is shifted 3.3 ppm upfield. In the heterocyclic bases, the C4 carbons are shifted more downfield than the C2 carbons. The C5 and C6 carbons move 60–90 ppm upfield as expected from the formation of the cyclobutane ring. The phosphorus–carbon coupling constants reported in Table III suggest conformational changes induced into the sugar–phosphate backbone during the conversion of UpU to *trans-syn*-U(p)U. The U(p)- $J_{pC2'}$, $J_{pC3'}$, and $J_{pC4'}$ all increase moderately in *trans-syn*-U(p)U. Along with these increases is a very significant reduction in -(p)U $J_{p5'C4'}$ from 8.7 to 3.6 Hz, reflecting changes in bond β(O5′–C5′) upon photodimer formation.

As observed in the ^1H NMR parameters, a comparison of the carbon-13 NMR parameters between these UpU photodimers indicates a significant difference between *cis-syn*-U(p)U and *trans-syn*-U(p)U. The chemical shift values of U(p)-C2′, -(p)U C1′, and -(p)U C5′ are grossly dissimilar in both photoproducts. Initial inspection of the coupling constants ($J_{pC2'}$, $J_{pC3'}$, and $J_{p5'C4'}$) for both *cis-syn*- and *trans-syn*-U(p)U also reveals contrasting values, thus implying a qualitative difference in the sugar–phosphate backbone conformation of these photodimers.

Discussion

Photochemical conversion of UpU to photodimers and subsequent isolation by HPLC have enabled the initiation of solution conformational investigations of entities responsible for distorting the secondary structure of model RNA helices. Acetone-photosensitized UV irradiation of UpU gives rise to four new resonances having different ^{31}P NMR chemical shift positions (Table I). Photodimers are identified by their formation by using sensitized conditions and their reversal to UpU upon reirradiation with 254-nm light. The four photodimers labeled U(p)U-1, U(p)U-2, U(p)U-3, and U(p)U-4 form in a ratio of 7.7:1.2:1.1:1.0 (Table I). Brown et al. (1966) observed three chromatographically separable UpU photodimers in a ratio of 6:2:1 after irradiation with 265-nm light. Considering the difficulties with the chromatographic separation of U(p)U isomers encountered in this work, the possibility cannot be excluded that comigration of two isomers occurred for Brown et al. (1966). In view of this, both the results of Brown et al. (1966) and those reported here are reasonably consistent. The U(p)U ^{31}P NMR resonances possess smaller temperature-dependent chemical shift values relative to UpU. These small values are expected from a reduction in the ability of α(P–O5′) and ζ(O3′–P) to attain nongauche conformations due to the rigidity imposed on the sugar–phosphate backbone by the cyclobutane ring.

The identification of U(p)U-1 as the *cis-syn*-U(p)U isomer is consistent with the observed ^1H, ^{13}C, and ^{31}P NMR parameters (Tables II, III, and I). Many proton spectral changes are similar in the formation of *cis-syn*-dT(p)dT, -dT(p)dU, and -U(p)U photodimers, namely, the upfield shifts of both H1′ protons, the downfield shift of the U(p)- H2′, and the slight upfield shift of the U(p)- H5′ and H5″. The upfield shift of the U(p)- H1′ (1.03 ppm) is very large compared to that observed in *cis-syn*-dT(p)dT (0.52 ppm) and is attributed to a greater change in the χ(C1–N1) glycosyl angle (Giessner-Prette & Pullman, 1977) as well as a possible inductive effect from a nearby oxygen. The downfield shift of the dT(p)-H2′ (Hruska et al., 1975) has been attributed to a conformational change from anti to syn in χ(C1′–N1) such as the one observed in the crystal structure of *cis-syn*-dT(p)dT cyanoethyl ester (Cadet et al., 1985). A similar downfield shift for U(p)- H2′ in *cis-syn*-U(p)U implies a high-anti or syn glycosyl conformation consistent with the interpretation of Hruska et al. (1985).

Considerable alterations are induced into both ribofuranose moieties in *cis-syn*-U(p)U by the formation of the cyclobutane ring. The proton-coupled ^{13}C patterns for the C2 carbons (Figure 4) qualitatively indicate dissimilar glycosyl orientations in the U(p)- and -(p)U nucleotides. The large $J_{1'2'}$ and small $J_{3'4'}$ values (Table II) in U(p)- and -(p)U suggest a preponderance of the C2′-endo sugar pucker. Furanose equilibria distributions have been calculated by using two approaches for *cis-syn*-U(p)U and UpU (Table IV). First, the percent of C2′-endo and C3′-endo distributions were determined by using the relationship developed initially by Altona and Sundaralingam (1973) and later modified by Alderfer and Ts'o (1977). It can be observed by using this method that both

Table V: Calculated Conformations of UpU, *cis-syn*-U(p)U, and *trans-syn*-U(p)U

	γ(C5′–C4′)[a]			β(O5′–C5′)[b]			ϵ(C3′–O3′)[c]			
	g^+	t	g^-	t	g^+	g^-	g^-	t	H3′,P (deg)	C4′,P[b] (deg)
UpU										
Up-	0.76	0.20	0.04				0.46	0.51	±28	212, 268
-pU	0.84	0.12	0.04	0.75 (0.78)[d]	0.10	0.10				
cis-syn-U(p)U										
U(p)-	0.71	0.16	0.13				0.96	0.04	±75	165, 315
-(p)U	*e*	*e*	*e*	0.72 (0.67)[d]	0.00	0.28				
trans-syn-U(p)U										
U(p)-	0.94	0.04	0.02				0.42	0.61	±17	223, 257
-(p)U	0.68	0.26	0.06	0.54 (0.30)[d]	0.14	0.32				

[a] Karplus-type equation used: $J_{HH} = 10.5 \cos^2 \phi - 1.2 \cos \phi$ (Altona & Sundaralingam, 1973) and rotamer equations from Davies and Danyluk (1974). [b] Equation used: $J_{HP} = 15.3 \cos^2 \phi - 6.1 \cos \phi + 1.6$ (Lankhorst et al., 1984) and rotamer equations from Davies and Danyluk (1974). [c] Equations used: $f_{g^-} = (J_{pC2'} - 1.0)/9.2$; $f_t = J_{pC4'}/9.2$ (Alderfer & Ts'o, 1977). [d] Equation used: $f_t = (J_{p5'C4'} - 0.73)/10.27$; $J_{CP} = 6.9 \cos^2 \phi - 3.4 \cos \phi + 0.7$ from Lankhorst et al. (1984). [e] Value not calculated because severe resonance overlap inhibited accurate $J_{4'5'}$ and $J_{4'5''}$ determination.

fragments of UpU maintain a C2′-endo/C3′-endo blend with a slight bias toward the C3′-endo pucker (56–57%). On the other hand, the *cis-syn*-U(p)- furanose is almost exclusively C2′-endo (91%) and the -(p)U ribose emphasizes the C2′-endo distribution (68%). In the other approach, the refined furanose sampling constants (Table II) are used as input data for analysis by PSEUROT.[3] The output of this program is the best fit conformation of a two-state equilibrium (Table IV) and the errors between the calculated and observed coupling constants. From this method, the distribution for the U(p)-nucleotide in *cis-syn*-U(p)U is 100% C2′-endo type while the -(p)U nucleotide is 100% C1′-exo. A similar calculation for UpU (Table IV) reveals a more even blend of 57% C2′-exo ↔ 43% C2′-endo type for the Up- fragment and 59% C2′-exo ↔ 41% C2′-endo type for -pU. These alterations in furanose equilibria might have conformational effects on neighboring nucleotides in a helix and thus result in intrastrand distortion.

The exocyclic bonds γ(C5′–C4′), β(O5′–C5′), and ϵ(C3′–O3′) in *cis-syn*-U(p)U are interpreted in terms of freely converting rotamer distributions and compared with those for UpU in Table V. The populations for γ(C5′–C4′) in U(p)- are similar to those in UpU; photodimer formation resulted in only a 5% decrease in the g^+ rotamer. An absence of refined -(p)U $J_{4'5'}$ and $J_{4'5''}$ values does not allow calculation of populations for the same bond in -(p)U. The trans rotamer for exocyclic bond β(O5′–C5′) is equally populated in UpU as in *cisy-syn*-U(p)U. It is apparent from the very small $J_{p5'}$ (2.38 Hz) that the g^- conformer around β(O5′–C5′) is virtually nonexistent. However, the large $J_{p5''}$ (8.14 Hz) translates into a large g^+ distribution (28%) for β(O5′–C5′). In the event the -(p)U H5′ and H5″ protons have been misassigned, the effect would be to interchange the distributions of g^+ and g^- in β(O5′–C5′). Contrary to the close similarity of γ(C5′–C4′) and β(O5′–C5′) in both UpU and *cis-syn*-U(p)U, the distributions around ϵ(C3′–O3′) are markedly different. UpU shows a near-equal blend of g^- and t conformers for ϵ(C3′–O3′) whereas the very small $J_{p3'C4'}$ (<0.5 Hz) and large $J_{pC2'}$ (8.8 Hz) (Table III) indicates an almost exclusive g^- population. Additional evidence for a significantly different phosphodiester region in *cis-syn*-U(p)U relative to UpU is the very small $J_{p3'}$ (1.1 Hz) and the rare occurrence of a large four-bonded U(p)-$J_{p2'}$ (2.95 Hz). The small ^{31}P NMR chemical shift dependence with temperature for *cis-syn*-U(p)U indicates reduced motional degrees of freedom in the phosphodiester region probably due to the presence of the cyclobutane ring.

[3] PSEUROT: Computer-Assisted Pseudorotational Analysis of Five-Membered Rings by Means of Vicinal Proton Spin–Spin Coupling Constants: Quantum Chemistry Program Exchange, Program No. 463, Indiana University.

Table VI: Rigid-Angle Analysis of Exocyclic Bonds in UpU Photodimers

	cis-syn-U(p)U			*trans-syn*-U(p)U		
coupling constant	Hz	Karplus angles (deg)	dihedral angles (deg)	Hz	Karplus angles (deg)	dihedral angles (deg)
			U(p)- γ(C5′–C4′)[a]			
$J_{4'5'}$	3.31	±51	171, 69	2.18	±58	178, 62
		±120	240, 0		±113	233, 7
$J_{4'5''}$	3.59	±49	49, 311	2.45	±57	57, 303
		±122	122, 238		±115	115, 245
av			239 ± 1			59 ± 2
			U(p)- ϵ(C3′–O3′)[b]			
$J_{pC2'}$	8.8	±149	269, 331	4.9	±124	244, 356
$J_{p3'C4'}$	0.5	±64	64, 296	5.7	±129	129, 231
		±86	86, 274			
$J_{p3'}$	1.03	±75	315, 165	9.74	±17	257, 223
		±81	321, 159		±123	3, 117
av			315 ± 14			232 ± 9 or 244 ± 11
			-(p)U γ(C5′–C4′)[a]			
$J_{4'5'}$	*c*	*c*	*c*	2.63	±55	175, 65
					±116	236, 4
$J_{4'5'}$	*c*	*c*	*c*	4.55	±44	44, 316
					±127	127, 233
av						234 ± 1
			-(p)U β(O5′–C5′)[b]			
$J_{pH5'}$	2.38	±59	179, 61	9.07	±22	142, 98
		±95	215, 25		±121	241, 359
$J_{pH5''}$	8.14	±28	268, 212	5.16	±43	283, 197
		±118	358, 122		±108	348, 132
$J_{p5'C4'}$	7.6	±141	141, 219	3.6	±19	19, 341
					±116	116, 244
av			215 ± 3			130 ± 11

[a] Karplus-type equation from Altona and Sundaralingam (1973): $J_{HH} = 10.5 \cos^2 \phi - 1.2 \cos \phi$. [b] Karplus-type equations used from Lankhorst et al. (1984): $J_{HP} = 15.3 \cos^2 \phi - 6.1 \cos \phi + 1.6$. $J_{CP} = 6.9 \cos^2 \phi - 3.4 \cos \phi + 0.7$. [c] Value not calculated because severe resonance overlap inhibited accurate $J_{4'5'}$ and $J_{4'5''}$ determination.

The conformational properties of the exocyclic bonds in *cis-syn*-U(p)U may not be best described as freely converting rotamers because of a high potential for restricted rotation due to photodimerization of the bases. The almost exclusive g^- population for ϵ(C3′–O3′), the absence of minor g^- conformers for β(O5′–C5′), the exclusive C2′-endo U(p)- ribofuranose, and predominant C2′-endo (or C1′-exo) furanose distribution in -(p)U, in addition to the small temperature-dependent ^{31}P chemical shift value, suggest the exocyclic bonds may be more appropriately analyzed in rigid angular terms. The proton–proton, proton–phosphorus, and carbon–phosphorus coupling constants observed in *cis-syn*-U(p)U were used to determine fixed conformational parameters in the exocyclic regions by

using Karplus-type relationships; the dihedral angles for *cis-syn*-U(p)U are listed in Table VI. The dihedral angle about γ(C5′–C4′) is determined from $J_{4'5'}$ and $J_{4'5''}$. The U(p)- $J_{4'5'}$ (3.31 Hz) and $J_{4'5''}$ (3.59 Hz) translate into ϕ(H4′,H5′) = ±51° (or ±120°) and ϕ(H4′,H5″) = ±49° (or ±122°), respectively. The best combination gives a O5′C5′–C4′C3′ dihedral angle of 239° (in the g^- class), which corresponds although poorly to 295° observed by Cadet et al. (1985) for *cis-syn*-dT(p)-. Optimal approximation of the dihedral angle about C3′–O3′ requires three coupling constants ($J_{pC2'}$, $J_{p3'C4'}$, and $J_{pH3'}$). The $J_{pC2'}$ (8.8 Hz), $J_{p3'C4'}$ (<0.5 Hz), and $J_{p3'}$ (1.08 Hz) translate into ϕ(C2′,P) = ±149°, ϕ(C4′,p) = ±64° (or ±86°), and ϕ(H3′,P) = ±75° (or ±81°) for ϵ(C3′–O3′). The best fit combinations include −149°, −64°, and either +75° or +81°, which convert into a C4′C3′–O3′P dihedral angle range of 314–316°. Consistent with the magnitudes of these three couplings is the large observable four-bonded $J_{p2'}$ (2.95 Hz). This range for ϵ(C3′–O3′) is in the g^- domain. The remaining exocyclic bond β(O5′–C5′) is best obtained by using $J_{p5'}$, $J_{p5''}$, and $J_{p5'C4'}$. For β(O5′–C5′), $J_{p5'}$ = 2.38 Hz, $J_{p5''}$ = 8.14 Hz, and $J_{p5'C4'}$ = 7.6 Hz, which translate into ϕ(H5′,P) = +59° (or ±95°), ϕ(H5″, P) = ±28° (or ±118°), and ϕ-(C4′,P) = ±141°. A very consistent solution involves the angles +95°, −28°, and −141°, which convert into a PO5′–C5′C4′ dihedral range of 215 ± 3°, an angle in the trans domain.

A critical comparison of the cyclobutane ring geometry of the *cis-syn*-dT(p)dT and -U(p)U photodimers cannot be made although differences are able to be inferred by examining the H6 chemical shift positions and the J_{66} value. The difference in chemical shift values between H6 protons in *cis-syn*-dT-(p)dT is small (0.072 ppm) compared to that for the same protons in *cis-syn*-U(p)U (0.396 ppm). This discrepancy suggests the environment around the H6 protons in U(p)U is much different from those in the deoxy photodimer. The observation of a 5.9–6.1-Hz J_{66} value for *cis-syn*-dT(p)dT (Hruska et al., 1975) compared to a J_{66} value of between 4.8 and 5.2 Hz observed by Hollis and Wang (1967) for Thy<>Thy and by Anet (1965) for DMT<>DMT led Hruska et al. (1975) to suggest that dT(p)dT has a flattened cyclobutane ring. Since the J_{66} in *cis-syn*-dT(p)dT is larger than the same coupling constant in *cis-syn*-U(p)U (4.86 Hz; Table II), it is consistent to state that the cyclobutane ring in *cis-syn*-U(p)U is not as flat as the ring in *cis-syn*-dT(p)dT. Steric repulsion of proximal methyl groups may be responsible for such a ring structure.

Identification of U(p)U-2 as a photodimer possessing a trans-syn cyclobutane configuration is consistent with its ^{31}P chemical shift position (Table I) and the proton NMR parameters in common with trans-syn I dT(p)dT (Liu & Yang, 1978). Formation of *trans-syn*-U(p)U has a major effect on the proton chemical shift values of the -(p)U fragment. The large upfield shift of the H1′ is similar in magnitude to the change in the -(p)U fragment of trans-syn II dT(p)dU (Liu & Yang, 1978) and is very consistent with a change in the χ(C1′–N1) angle as suggested by Giessner-Prette and Pullman (1977). Another consistency between these trans-syn models is the change in the chemical shift value (0.04 ppm) of the U(p)- H1′ and the very small shift for the dT(p)- H1′ (Liu & Yang, 1978). Upfield shifts of similar magnitude for both H4′ protons are observed in the fragments of *trans-syn*-U(p)U and trans-syn II dT(p)dT. Finally, the large displacements of the four base protons, H5 and H6, and base carbons, C5 and C6, to higher field are characteristic of C5=C6 saturation in pyrimidines due to the formation of the cyclobutane ring.

A more descriptive account of the conformational changes induced into *trans-syn*-U(p)U is obtained by using the proton coupling constants. The extremely small $J_{1'2'}$ and large $J_{3'4'}$ (Table II) for both furanose systems indicates the sugar pucker equilibria are almost exclusively C3′-endo. The percent C2′-endo/C3′-endo distributions are calculated for *trans-syn*-U(p)U and compared to those for UpU in Table IV. In contrast to the usual C2′-endo/C3′-endo blend for UpU, the *trans-syn*-U(p)- furanose is exclusively C3′-endo (97%) and the -(p)U moiety is predominantly a C3′-endo pucker (84%). The furanose conformation calculated from $J_{1'2'}$, $J_{2'3'}$, and $J_{3'4'}$ by using PSEUROT indicates 100% C3′-endo for *trans-syn*-U(p)- and 100% C3′-endo type for the -(p)U nucleotide.

Changes in the coupling constants of the *trans-syn*-U(p)U exocyclic bonds reveal considerably different rotamer distributions relative to UpU (Table V). The populations for γ-(C5′–C4′) in U(p)- are almost solely g^+ (94%) compared with 76% in UpU. By contrast, a high proportion of trans rotamers (26%) and a reduced amount of g^+ conformers (68%) exist in the -(p)U fragment compared with predominantly g^+ conformers (84%) in UpU. Photodimer formation appears to have altered the distributions in another exocyclic bond, β(O5′–C5′). The trans rotamers are reduced from 75% to 54% while the g^+ rotamer increases nearly 15%. An inconsistency is observed in the distributions of the trans rotamer for O5′–C5′ calculated from the proton–phosphorus coupling constants (Table II) and the $J_{p5'C4'}$ (Table III). The formation of the trans-syn cyclobutane ring has a minimal effect upon the remaining exocyclic bond, ϵ(C3′–O3′).

The constraint of the trans-syn cyclobutane ring in U(p)U is believed to restrict conformational mobility of some exocyclic and endocyclic bonds in the sugar–phosphate backbone as evident from the proportions of rotamer populations as well as preponderance of the C3′-endo furanose distributions in both nucleotides. Therefore, the exocyclic bonds of *trans-syn*-U-(p)U were evaluated in rigid angular terms in a manner similar to the treatment of *cis-syn*-U(p)U (see Table VI). For U(p)-, $J_{4'5'}$ (2.18 Hz) and $J_{4'5''}$ (2.45 Hz) translate into ϕ(H4′,H5′) = ±58° (or ±113°) and ϕ(H4′,H5″) = ±57° (or ±115°). Since the chemical shift values of the U(p)- H5′,H5″ change insignificantly upon photodimer formation compared to those in *cis-syn*-U(p)U, the γ(C5′–C4′) dihedral angle is not expected to undergo a dramatic reorientation to the g^- region as proposed for *cis-syn*-U(p)U. Therefore, the most likely combination is −58° and +57°, which gives a O5′C5′–C4′C3′ dihedral angle of 59°, a conformation in the $gauche^+$ domain. In the case of exocyclic bond ϵ(C3′–O3′), the $J_{pC2'}$ (4.9 Hz), $J_{p3'C4'}$ (5.7 Hz), and $J_{p3'}$ (9.74 Hz) convert to ϕ(C2′,P) = ±124°, ϕ(C4′,P) = ±129°, and ϕ(H3′,P) = ±17° (or ±123°). The best combination is +124°, −129°, and −17°, which gives C4′C3′–O3′P dihedral angles of 224°, 231°, and 223°, respectively. The average of these values is 232°, which is a ϵ(C3′–O3′) dihedral angle in the trans class but is very close to the g^- domain. The conformation about β(O5′–C5′) is determined from $J_{p5'}$ (9.07 Hz), $J_{p5''}$ (5.16 Hz), and $J_{p5'C4'}$ (3.6 Hz). These coupling constants translate into ϕ(H5′,P) = ±22° (or ±121°), ϕ(H5″,P) = ±43° (or ±108°), and ϕ(C4′,P) = ±19° (or ±116°). The structurally possible combination is +22°, −108°, and +116°, which yeilds PO5′–C5′C4′ dihedral angles of 116–142°; the average value is 130°, which is a conformation bordering the trans and $gauche^+$ domains. Finally, in rigid terms, bond -(p)U γ(C5′-C4′) is determined from $J_{4'5'}$ (2.63 Hz) and $J_{4'5''}$ (4.55 Hz), which translate into ϕ(H4′,H5′) = ±55° (or ±116°) and ϕ(H4′,H5″) = ±44° (or ±127°), respectively. The best combination gives an

O5′C5′–C4′C3′ dihedral angle of 234 ± 1°, which lies in the g^- domain, a significant change from the predominant g^+ distribution.

A comparison of the conformational properties of both U(p)U photodimers shows many contrasting features. The different base–base configurations are reflected in the variety of H5–H5, H5–H6, and H6–H6 coupling constants (Table II). The furanose distributions in *cis-syn*-U(p)U are dominated by S-type puckers while both *trans-syn*-U(p)U ribose systems are exclusively N-type puckers (Table IV). The rotamer distribution around U(p)– γ(C5′–C4′) in *trans-syn*-U(p)U is almost entirely g^+ (94%) whereas contributions from other rotamers are observed in *cis-syn*-U(p)U. The lack of calculated populations for -(p)U γ(C5′–C4′) in the cis-syn isomer precludes a comparison of this important torsion angle between the cyclobutyl-linked bases. A substantial decrease in the trans population for β(O5′–C5′) in *trans-syn*-U(p)U occurs relative to *cis-syn*-U(p)U (Table V). In corroboration, the rigid-angle evaluation shows a PO5′–C5′C4′ dihedral angle of 215 ± 3° for *cis-syn*-U(p)U and 130 ± 11° for the trans-syn isomer. Moreover, the ϵ(C3′–O3′) in *cis-syn*-U(p)U is almost exclusively g^- (96%); by contrast, the major contribution in the trans-syn isomer around the same bond comes from the trans domain (61%). Finally, the dihedral angle around C4′C3′–O3′P is 315 ± 14° for *cis-syn*-U(p)U and 232 ± 9° for *trans-syn*-U(p)U. It can be speculated that the contrasting structural features of the -(p)U furanose and U(p)- exocyclic bond γ(C5′–C4′) in both photodimers induces nucleotides adjacent to these lesions to have dissimilar conformational properties. Consequently, a variety of distortion in a RNA helix may result from photodimers possessing different cyclobutane ring configurations.

ACKNOWLEDGMENTS

We thank Dr. Harold C. Box for the use of his preparative HPLC facility and Peter Demou at the Chemical Instrumentation Center, Yale University, and Dr. Alex D. Bain and Dr. Charles Roger at Bruker Spectrospin (Canada) Ltd., Milton, Ontario, for recording the 500-MHz proton NMR data.

Registry No. UpU, 2415-43-2; *cis-syn*-U(p)U, 113490-66-7; acetone, 67-64-1.

REFERENCES

Adman, E., & Jensen, L. (1970) *Acta Crystallogr., Sect. B: Struct. Crystallogr. Cryst. Chem. B26*, 1326–1334.

Alderfer, J. L., & Ts'o, P. O. P. (1977) *Biochemistry 16*, 2410–2416.

Altona, C., & Sundaralingam, M. (1973) *J. Am. Chem. Soc. 95*, 2333–2344.

Anet, R. (1965) *Tetrahedron Lett. 42*, 3713–3717.

Bawden, F. C., & Klecskowski, A. (1959) *Nature (London) 183*, 503–504.

Bollum, F. J., & Setlow, R. B. (1963) *Biochim. Biophys. Acta 68*, 599–607.

Brown, I. H., Freeman, K. B., & Johns, H. E. (1966) *J. Mol. Biol. 15*, 640–662.

Broyde, S., Stellman, S., & Hingerty, B. (1980) *Biopolymers 19*, 1695–1701.

Burr, J. G. (1968) *Adv. Photochem. 6*, 193–299.

Cadet, J., Voituriez, L., Hruska, F. E., & Grand, A. (1985) *Biopolymers 24*, 897–903.

Chan, G. L., Doetsch, P. W., & Haseltine, W. A. (1985) *Biochemistry 24*, 5723–5728.

Cheng, D. M., & Sarma, R. H. (1977) *J. Am. Chem. Soc. 99*, 7333–7348.

Davies, D. B., & Danyluk, S. S. (1974) *Biochemistry 13*, 4417–4434.

Fisher, G., & Johns, H. E. (1976) in *Photochemistry and Photobiology of Nucleic Acids* (Wang, S., Ed.) Vol. 1, pp 226–289, Academic, New York.

Giessner-Prette, C., & Pullman, B. (1977) *J. Theor. Biol. 65*, 171–188.

Gordon, M. P., Huang, C., & Hurter, J. (1976) in *Photochemistry and Photobiology of Nucleic Acids* (Wang, S., Ed.) Vol. 2, pp 265–308, Academic, New York.

Gorenstein, D. G. (1978) in *Nuclear Magnetic Resonance Spectroscopy in Molecular Biology* (Pullman, B., D., Ed.) pp 1–15, Reidel, Dordrecht, Holland.

Greenstock, C. L., & Johns, H. E. (1968) *Biochem. Biophys. Res. Commun. 30*, 21–27.

Hall, R. K., & Larcom, L. L. (1982) *Photochem. Photobiol. 36*, 429–432.

Hariharan, P. V., & Johns, H. E. (1968) *Photochem. Photobiol. 8*, 11–22.

Hollis, D. P., & Wang, S. H. (1967) *J. Org. Chem. 32*, 1620–1622.

Hruska, F. E., Wood, D., Ogilvie, K., & Charlton, J. (1975) *Can. J. Chem. 53*, 1193–1203.

Hruska, F. E., Berger, M., Cadet, J., & Remin, M. (1985) *Can. J. Chem. 63*, 15–23.

Kan, L. S., Cheng, D. M., & Cadet, J. (1982) *J. Magn. Reson. 48*, 86–96.

Katritzky, A. R., Nesbit, M. R., Kurtev, B. J., Lyapova, M., & Pojarlieff, I. G. (1969) *Tetrahedron 25*, 3807–3824.

Kucan, Z., Wait, H. P., & Chambers, R. W. (1972) *Biochemistry 11*, 3290–3295.

Lankhorst, P. P., Haasnoot, C. A. G., Erklens, C., & Altona, C. (1984) *J. Biomol. Struct. Dyn. 1*, 1387–1405.

Lee, C.-H., Ezra, F. S., Kondo, N. S., Sarma, R. H., & Danyluk, S. S. (1976) *Biochemistry 15*, 3627–3639.

Liu, F. T., & Yang, N. C. (1978) *Biochemistry 17*, 4865–4876.

Radman, M., Villani, G., Boiteux, S., Kinsella, A. R., Glickman, B. W., & Spadari, S. (1977) *Cold Spring Harbor Symp. Quant. Biol. 43*, 937–946.

Remin, M., & Shugar, D. (1972) *Biochem. Biophys. Res. Commun. 48*, 636–642.

Rycyna, R. E., & Alderfer, J. L. (1985) *Nucleic Acids Res. 13*, 5949–5963.

Sarin, P. S., & Johns, H. E. (1968) *Photochem. Photobiol. 7*, 203–210.

Sauerbier, W. (1976) *Adv. Radiat. Biol. 6*, 49–106.

Setlow, R. B., Carrier, W. L., & Bollum, F. J. (1964) *Biochim. Biophys. Acta 91*, 446–461.

Shine, J., & Dalgarno, L. (1974) *Proc. Natl. Acad. Sci. U.S.A. 71*, 1342–1346.

Shuster, H. (1964) *Z. Naturforsch., B: Anorg. Chem., Org. Chem., Biochem. Biophys. Biol. 19B*, 815–830.

Steitz, J., & Jakes, K. (1975) *Proc. Natl. Acad. Sci. U.S.A. 72*, 4734–4738.

Varghese, A. J. (1972) *Photophysiology 7*, 207–274.

Wang, S. Y., Ed. (1976) *Photochemistry and Photobiology of Nucleic Acids*, Vols. 1 and 2, Academic, New York.